

¹R. Moreh and O. Shahal, Nucl. Phys. **A252**, 429 (1975).

²R. Moreh, O. Shahal, and V. Volterra, Nucl. Phys. **A262**, 221 (1976).

³O. Shahal and R. Moreh, Phys. Rev. Lett. **40**, 1714 (1978).

⁴W. E. Lamb, Phys. Rev. **55**, 190 (1939).

⁵J. K. Kjems *et al.*, Phys. Rev. Lett. **32**, 724 (1974), and Phys. Rev. B **13**, 1446 (1976).

⁶W. A. Steele, J. Phys. (Paris), Colloq. **38**, C4-61 (1977).

⁷S. Ostlund and A. N. Berker, Phys. Rev. Lett. **42**, 843 (1979).

⁸T. T. Chung and J. G. Dash, Surf. Sci. **66**, 559 (1977).

⁹A. J. Berlinsky and A. B. Harris, Phys. Rev. Lett. **40**, 1579 (1978).

¹⁰S. M. Heald and E. A. Stern, Phys. Rev. B **17**, 4069 (1978).

Electronic Raman Scattering and Antiresonance Behavior in Highly Stressed Photoexcited Silicon

D. Guidotti, Shui Lai, M. V. Klein, and J. P. Wolfe

Physics Department and Materials Research Laboratory, University of Illinois at Urbana-Champaign, Urbana, Illinois 61801

(Received 5 September 1979)

Inelastic light scattering from photoproduced carriers is observed in stressed high-purity silicon at low temperatures. The two electronic Raman structures observed correspond to transitions between stress-split valence bands at the zone center. These transitions can be stress-tuned to the Γ -point phonon energy, thereby exhibiting Fano-type interference between competing scattering amplitudes.

When intrinsic silicon is illuminated with light above the band gap, electron-hole (e-h) pairs are produced which, at low temperatures, bind into excitons near the surface of excitation. Application of uniform compressive stress parallel to the [001] crystallographic direction causes narrowing of the indirect gap and lowers the band energy of indirect excitons. If stress is applied through a spherical contact surface, the resulting nonuniform stress exhibits a relative maximum and, therefore, a potential-energy minimum for excitons inside the bulk. With use of this method of strain confinement, excitons are drawn from the surface, where they are produced by a pump laser, and collect in the strain well where condensation into an electron-hole liquid (EHL) occurs at low temperatures ($T \lesssim 15$ K).^{1,2} A feature of strain confinement is that a high concentration of e-h pairs may be created, with moderate excitation levels, in a nearly spherical volume approximately 100 μm in diameter and totally within the bulk of the sample. We probe the strain-confined exciton gas or EHL by inelastic light scattering using Nd-doped YAlO_3 (10 796 \AA) or yttrium aluminum garnet (10 644 \AA) lasers which have photon energies just below the silicon indirect band edge.

We observe, for the first time in elemental semiconductors, two Raman-active inter-valence-band transitions at the Γ point over a wide range of temperatures (1.8–68 K) and applied stress

(40–170 kg/mm^2). These transitions, labeled A and B in Fig. 1, shift with applied stress and thus provide a unique opportunity to tune each one to the $\Gamma_{25'}$ phonon energy. The antiresonance line shapes observed under these conditions are in good agreement with a modified Fano theory^{3,4} in which a transition to the discrete phonon state mixes with the finite continuum of inter-valence-band Raman transitions (A and B) through electron-phonon interaction. This coupling is simi-

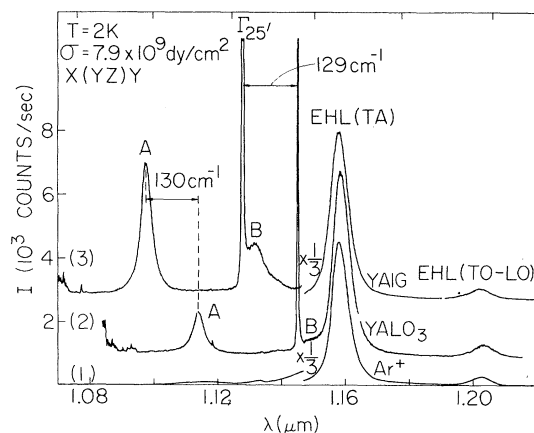


FIG. 1. Overall spectrum from strain well. (1) With argon-ion pump laser only, (2) with YAlO_3 probe laser plus the Ar^+ laser, and (3) with yttrium aluminum garnet probe laser plus the Ar^+ laser. The energy difference between the two probe lasers is 132 cm^{-1} .

lar to that observed between the $\Gamma_{25'}$ phonon and a broad continuum of $|V_1\rangle$ to $|V_2\rangle$ hole transitions in unstressed, heavily doped, *p*-type silicon.⁵ While in Ref. 5 the electronic continuum is not experimentally accessible, the present case involves a much simpler and fully characterized spectrum of electronic transitions.

We utilize a single crystal of high-purity dislocation-free silicon cut such that all faces are (100). Compressive [001] stress is applied with a steel rod, one end of which is a section of spherical surface of radius R , with $R = 0.95\text{--}6.1$ cm. Under these conditions, electrons and holes created at a (010) surface by an argon-ion laser are quickly drawn by the strain gradient into the region of high strain (transit time $\sim 1 \mu\text{s}$ at 2 K), where thermalization occurs prior to recombination, and EHL is formed when $T \lesssim 15$ K.^{1,12}

Theoretical⁶ and experimental¹ considerations suggest that with a spherical stressing geometry, we should expect a nearly uniform and uniaxial stress over a small volume about the stress maximum. This is verified in our case, where the EHL luminescence displays no strain broadening. The actual stress at the EHL site is determined by measuring the luminescence spectral shift which is then fitted to previous uniform-stress data.^{7,8}

With use of a conventional 90° scattering geometry with z as the stress axis, both inelastically scattered light and recombination luminescence are analyzed by a single-grating 0.5-m Spex spectrometer and detected by photon-counting techniques with a Varian VPM-164 photomultiplier tube. Typical recorder traces for applied stress $8 \times 10^9 \text{ dyn/cm}^2$ and $T = 2$ K are shown in Fig. 1. With only the Ar^+ pump laser on, the observed spectrum, trace 1, contains TA and LO-TO phonon-assisted EHL recombination luminescence emanating from the potential well. At high stresses, LO-TO luminescence becomes totally polarized perpendicular to the stress axis, while the TA peak remains partially polarized, making the LO-TO replica appear much weaker. Detailed discussion of these observations will be the subject of a subsequent paper. With the simultaneous operation of the probe beam carefully focused on the strain well (traces 2 and 3), we observe new Raman transitions A and B in addition to the usual zone-center optical phonon. The Raman nature of these new peaks is evident from their spectral shift when the probe-laser frequency is changed by 132 cm^{-1} . Unlike the Γ -point phonon, the intensity of A and B is found to be proportional to

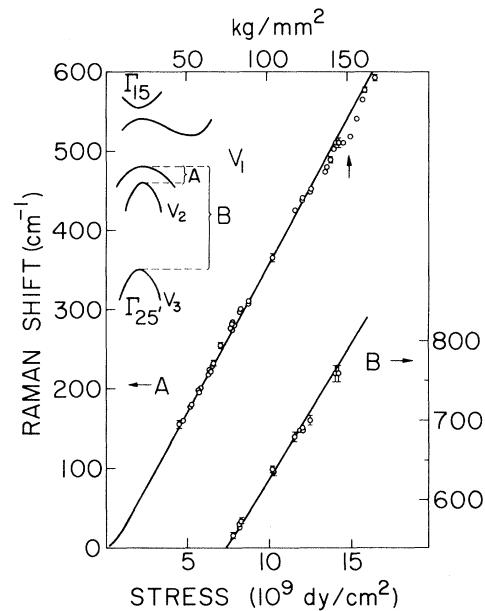


FIG. 2. Stress dependence of the peak position of A and B transitions. The solid lines are shifts calculated from Eqs. (1). The inset indicates band splittings under stress and the vertical arrow indicates stress at which A overlaps with the phonon.

the number of e-h pairs in the well, therefore establishing their electronic origin.

We have looked for, but find no evidence of, scattering from plasma oscillations. We estimate a plasma frequency $\omega_p \approx 120 \text{ cm}^{-1}$ for the strain-confined EHL and a scattering efficiency about 10^{-3} times that of the Γ phonon, corresponding to an integrated intensity of about 10 counts/s in our experiment.

Spectral variation of both A and B lines with stress, Fig. 2, is consistent with their assignment to electronic transitions between stress-split valence-band states. Thus A is identified, in the $|J, m_j\rangle$ total-angular-momentum representation, as a transition from $|V_2\rangle = |j_{\frac{3}{2}}, \frac{3}{2}\rangle$ (light-hole band) to the stress-mixed state $|V_1\rangle = a|j_{\frac{3}{2}}, \frac{1}{2}\rangle - b|j_{\frac{1}{2}}, \frac{1}{2}\rangle$ (heavy-hole band), and B is consistent with electronic transitions from the spin-orbit-split band $|V_3\rangle = b|j_{\frac{3}{2}}, \frac{1}{2}\rangle + a|j_{\frac{1}{2}}, \frac{1}{2}\rangle$ to empty states in $|V_1\rangle$. The mixing coefficients a and b depend on stress.^{9,10} From our observed polarization intensities we conclude that both types of transitions seem to proceed via nearly direct virtual transitions to *p* states in the Γ_{15} conduction band. Observed and computed selection rules are stress dependent because of stress-induced mixing of $m_j = \frac{1}{2}$ states and are summarized in Table I for a stress

TABLE I. Observed (calculated) polarization selection rules.

	YZ/YX	ZZ/ZX	YZ/ZX
<i>A</i>	10 (90 ± 60)	1/20 (0)	~1 (1)
<i>B</i>	20 (1/0)	1/20 (1/50)	~1 (1)

of 10^{10} dyn/cm². Our crossed analyzer-polarizer extinction ratio was measured to be 22:1. The spread in the calculated ratio YZ/YX for *A* is a consequence of the uncertainty with which the deformation potentials are known.⁹ It should be noted that *A* is strictly forbidden in (*ZZ*) symmetry, while *B* is symmetry allowed in (*ZZ*) but is very weak; ($ZX:ZZ$)_{expt} ≥ 50:1, while experimentally ($ZX:ZZ$)_{expt} = 20:1.

The stress-dependent valence-band splittings can be written in terms of deformation-potential parameters b_1 and b_2 ^{9, 10}:

$$V_1 - V_2 = -\frac{1}{2}(\Delta_0 + \frac{1}{2}\delta_1) - [(\Delta_0 - \frac{1}{2}\delta_1)^2 + 2\delta_2^2]^{1/2}, \quad (1)$$

$$V_1 - V_3 = [(\Delta_0 - \frac{1}{2}\delta_1)^2 + 2\delta_2^2]^{1/2},$$

where $\delta_1 = 2(b_1 + 2b_2)(S_{11} - S_{12})X$, $\delta_2 = 2(b_1 - b_2)(S_{11} - S_{12})X$, $\Delta_0 + 0.044$ eV is the spin-orbit splitting, X is the applied [001] stress, and S_{11} and S_{12} are elastic compliance constraints.⁹ In Fig. 2 the stress dependence of valence-band splittings predicted by Eqs. (1) is compared with Raman shifts of *A* and *B*. Deformation-potential parameters consistent with our measured shifts are $b_1 = -1.56 \pm 0.05$ eV and $b_2 = -0.06 \pm 0.05$ eV. These values are 18% lower than those obtained from infrared (ir) absorption measurements on *n*-type silicon.⁹ This difference is probably representative of uncertainties in the absolute value for the applied stress in uniform-stress measurements.

The spectral line shapes of the new Raman transitions are not quantitatively understood. The *A* line is fitted well by a simple Lorentzian with full width at half maximum = 4 MeV, nearly 3 times broader than the spectrum obtained by simply considering vertical transitions between the two hole bands with a Fermi distribution of holes in the EHL. The Lorentzian character of the *A* line suggests lifetime broadening due to a scattering mechanism with relaxation time $\tau = 0.18$ ps.

The ability to tune the electronic Raman transitions with stress allows a unique opportunity to study interference between the scattering amplitude of a discrete state (the $\Gamma_{25'}$ phonon) and that

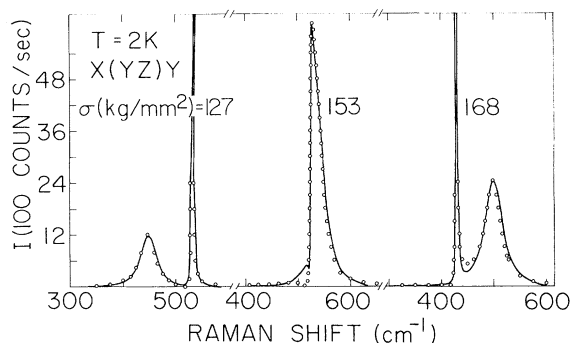


FIG. 3. Stress tuning of antiresonance. The solid lines are experimental traces normalized for system's response. Circles represent the line shape calculated from Eq. (2). Note the marked asymmetry at maximum overlap.

of completely experimentally characterized continua of electronic excitations represented by the *A* and *B* lines. In what follows we consider only interference between *A* and the Γ phonon.

The symmetry of the zone-center optical phonon in silicon is the same as that of a pure [111] shear strain, namely $\Gamma_{25'}$. The Raman tensor for *A* transitions also has the same symmetry, and Fano-type antiresonance behavior is observed in all polarizations attainable in our scattering geometry. The effect is shown in Fig. 3 at three representative stresses. As [001] stress is increased and the high-energy tail of the *A* transitions visibly overlaps with the Γ phonon, it becomes possible for holes to make $|V_1\rangle \leftrightarrow |V_2\rangle$ transitions by directly absorbing or emitting an optical phonon, in addition to the Raman process. We then observe a decrease in the peak intensity of both lines with marked broadening of the phonon on the high-energy side. At maximum overlap, the mixed line has about one-fourth the original peak intensity of the phonon and nearly three times that of the noninteracting *A* line. At higher stresses, the two Raman transitions again separate and return to peak intensities close to their original values. Throughout these changes in line shape, the integrated intensity of the spectrum remains constant with 10%. This behavior is well described by a modified Fano analysis of discrete-continuum interaction with line shape given by⁴

$$I = D \frac{\pi \rho(E) T_e^2 (E_0 - E - r)^2}{[E_0 - E + V^2 R(E)]^2 + \pi^2 V^4 \rho^2(E)}, \quad (2)$$

where $r \equiv VT_p/T_e$, and T_e and T_p are the Raman transition amplitudes (assumed real) for *A* and

the phonon, respectively. E_0 is the phonon energy, V is the electron-phonon interaction, $\rho(E)$ and $R(E)$ are the density of states and spectral response of A transitions, and D is a scale factor.

Because of the Lorentzian character of A when far away from the phonon, we use the complex response function

$$G_e = \frac{C}{E_e - E - i\gamma/2} \quad (3)$$

to describe the spectrum of electronic transitions. Then $\pi\rho(E) = \text{Im}G_e$ and $R(E) = \text{Re}G_e$. C can be interpreted as the number of holes per unit cell, whereas E_e and γ are the peak position and the full width at half maximum of A , respectively. A more microscopic theory of interference line shapes may be found elsewhere.^{11,12}

We can estimate the magnitude of the pertinent parameters as follows. When A is sufficiently removed from the phonon, we obtain $\gamma = 34 \pm 3 \text{ cm}^{-1}$ independent of stress and $E_0 = 527 \pm 1 \text{ cm}^{-1}$. The ratio of the integrated intensity of A to that of the phonon when both are well separated, is obtained from Eq. (2); $g = (T_e/T_p)^2 C$. Experimentally, we find $g = 1.0 \pm 0.2$. From the ratio of peak intensities of A before and after the phonon, we also determine $r = 13.0 \pm 0.2 \text{ cm}^{-1}$. Then from g and r we obtain $CV^2 = 170 \pm 30 \text{ cm}^{-2}$. As an upper limit of C we assume that the strain well contains EHL with average e-h pair concentration of $3.7 \times 10^{17} \text{ cm}^{-3}$.¹ Then $C = 1.5 \times 10^{-5}$ from which we obtain the electron-phonon interaction, $V = 420 \pm 35 \text{ meV}$, as well as $T_p/T_e = (4.0 \pm 0.4) \times 10^{-3}$. The uncertainty in these figures reflects the spread in γ which is due to experimental noise. It should be emphasized that all three spectra in Fig. 3 are fitted with the same parameter values given above, allowing only E_e , the spectral position of

the A peak, to be varied with stress.

In summary, we have observed new electronic Raman lines in optically pumped, stressed Si due to inter-valence-band hole excitations. The shift with stress, selection rules, and interference behavior of the new lines with optical phonons are reasonably well understood, allowing measurement of the electron-phonon interaction.

This work was supported by the National Science Foundation under Materials Research Laboratory Grants No. DMR-77-23999 and No. DMR-79-02780. We thank P. L. Gourley for very helpful discussions and E. E. Haller for providing us with the Si samples.

¹P. L. Gourley and J. P. Wolfe, Phys. Rev. Lett. **40**, 526 (1978).

²P. L. Gourley and J. P. Wolfe, Phys. Rev. B **20**, 3319 (1979).

³U. Fano, Phys. Rev. **124**, 1866 (1961).

⁴M. V. Klein, in *Light Scattering in Solids*, edited by M. Cardona (Springer-Verlag, Berlin, 1977).

⁵Fernando Cerdeira, T. A. Fjeldly, and M. Cardona, Phys. Rev. B **8**, 4734 (1973).

⁶R. S. Markiewicz, J. P. Wolfe, and C. D. Jeffries, Phys. Rev. B **15**, 1988 (1977).

⁷B. M. Ashkinadze, I. P. Kretsu, A. A. Patrin, and I. D. Yaroshetskii, Fiz. Tekh. Poluprovodn. **4**, 2206 (1970) [Sov. Phys. Semicond. **4**, 1897 (1971)].

⁸P. L. Gourley, unpublished.

⁹Lucien D. Laude, Fred H. Pollak, and Manuel Cardona, Phys. Rev. B **3**, 2623 (1971).

¹⁰H. R. Chandrasekhar, A. K. Ramdas, and Sergio Rodriguez, Phys. Rev. B **12**, 5780 (1975).

¹¹M. Balkanski, K. P. Jain, R. Beserman, and M. Jouanne, Phys. Rev. B **12**, 4328 (1975).

¹²I. P. Ipatova and A. V. Subashiev, Fiz. Tverd. Tela **18**, 2145 (1976) [Sov. Phys. Solid State **18**, 1251 (1976)].